Quasar Main Sequence

The physical driver of Eigenvector 1

3rd Cosmology School, Cracow-2017

Swayamtrupta Panda

Supervisor: Prof. Bożena Czerny

in collaboration with: Marzena Śniegowska, Conor Wildy, Krzysztof Hryniewicz

Nicolaus Copernicus Astronomical Center
&
Center for Theoretical Physics, Polish Academy of Sciences

Project Goal

The aim of the project is ”**to explain which combination of the natural physical AGN parameters (black hole mass, accretion rate, spin and inclination angle) is responsible for the Quasar Main Sequence in type 1 AGNs**”

Nicolaus Copernicus Astronomical Center
&
Center for Theoretical Physics, PAN

Motivation

In search for a equally robust scheme for studying the sequencing in quasars - An extension of the Hertzsprung-Russell diagram?

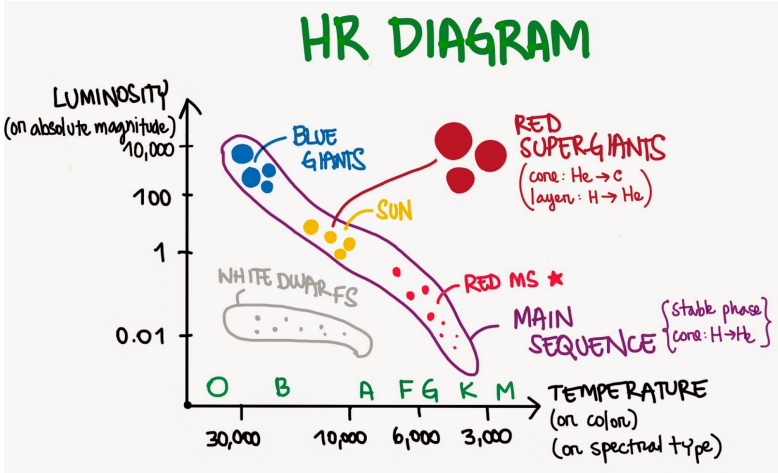

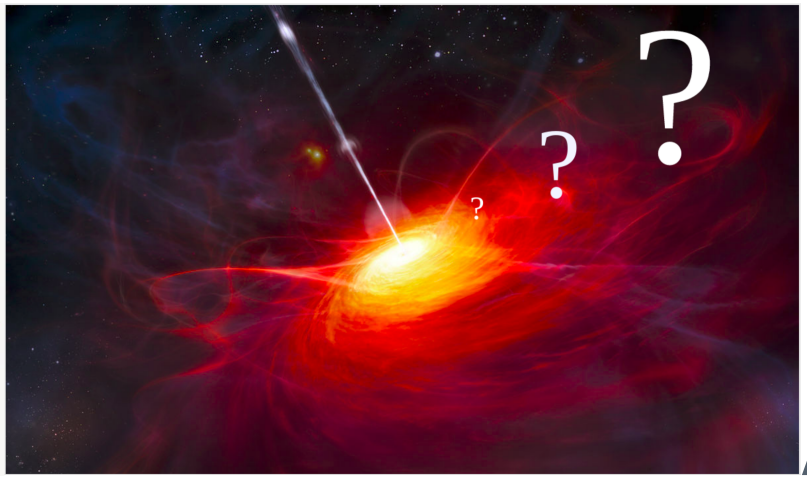

HR-like diagram for Quasars...

Nicolaus Copernicus Astronomical Center
&
Center for Theoretical Physics, PAN

Eigenvector 1

- Boroson & Green (1992) found a single parameter which was responsible for most of the dispersion in the observed properties of Type 1 AGNs - the **Eigenvector 1** (EV1)

- They perform the **Principal Component Analysis** (PCA) with 13 tabulated properties ($\mathrm{M_v}$, log R, α_{ox}, EW Hβ, R λ5007, R λ4686, **R Fe$_{\mathrm{II}}$**, Peak λ5007, **Hβ FWHM**, Hβ shift, Hβ shape, Hβ asymmetry, and, M$_{[\mathrm{OIII}]}$)

PCA Analysis Demo

Eigenvector 1

Anticorrelation between $\mathrm{Fe_{II}} - [\mathrm{OIII}]$ (r = -0.670)

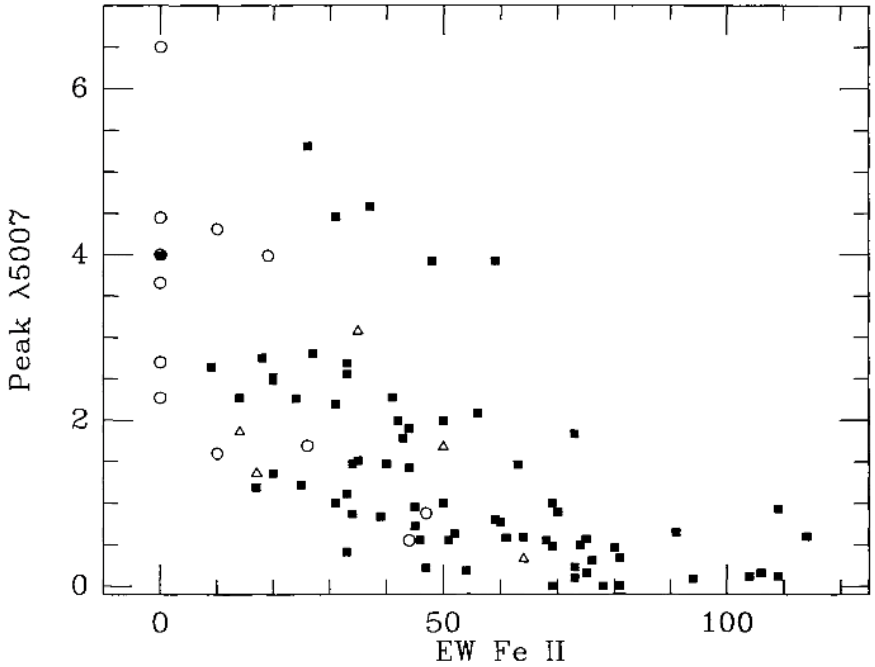

FIG. 2.—Ratio of peak height of [O III] λ5007 to that of Hβ plotted against equivalent width of the Fe II emission between λ4434 and λ4684. Solid squares are radio-quiet objects, open circles are steep-spectrum radio sources, and open triangles are flat-spectrum radio sources.

Distribution of quasars in the EV1 plane

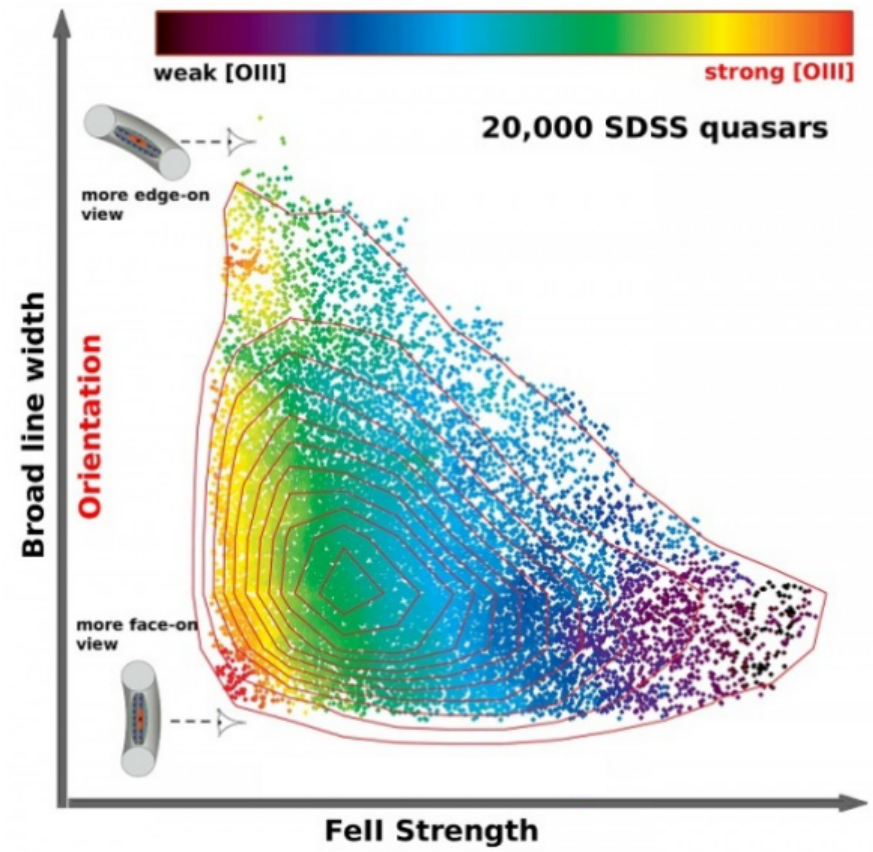

Figure: The distribution of the FWHM(Hβ) for 20,000 quasars plotted against the EV1. The horizontal axis is the relative Fe II strength ($R_{Fe_{II}}$) and the vertical axis is the broad Hβ FWHM. The red contours show the distribution of selected quasar sample (quasar density increasing from outer to inner contours). The points are color-coded by the [OIII] (λ = 5007Å) EW, averaged over all nearby objects in a smoothing box of ΔR_{Fe} = 0.2 and $\Delta FWHM_{H\beta}$ = 1,000 km/s.

The physical driver of EV1

"We postulate that the true driver of EV1 is the **maximum of the accretion disk temperature**, one that also determines the broad band shape of the quasar continuum emission"

From Theoretical Standpoint

- The use of a **two-component input spectra** is motivated by the fact that the quasar SED is indeed dominated by two physically different spectral components. Most of the quasar radiation comes from the accretion disk and forms the Big Blue Bump (BBB) in the optical-UV. This is parametrized by the mass of the black hole, the accretion rate, spin and the cosine of the inclination angle. The BBB, located around the Lyman edge ($\lambda = 1216$ Å) dominates the optical-UV emission and their total energy output

$$T_{max} = \left[\frac{3GM\dot{M}}{8\pi\sigma r^3}\left(1-\sqrt{\frac{R_{in}}{r}}\right)\right]^{0.25} = 2.034\times10^{19}\left(\frac{\dot{M}}{M^2}\right)^{0.25}$$

SED parametrization - Initial Assumptions

To model the AGN full continuum, the SED of a quasar is parametrized by:

1. a low-energy slope of the Big Bump continuum (α_{uv});
2. slope of the X-ray component (α_{x});
3. their corresponding exponential cutoffs;
4. the relative luminosities of these two components (determined by setting the spectral index α_{ox} , that describes the continuum between optical-UV bump and the X-ray peak);
5. incorporating a total bolometric luminosity (= 10^{45} erg s^{-1}) of the quasar cloud;
6. the position of the broad line region (R_{BLR}) from the core of the nuclei;
7. the mean hydrogen density ($\mathrm{n_H}$) of the cloud (deduced from the ratios of emission lines); and
8. a limiting column density ($\mathrm{N_H}$) to define the outer edge of the cloud.

SED Modeling

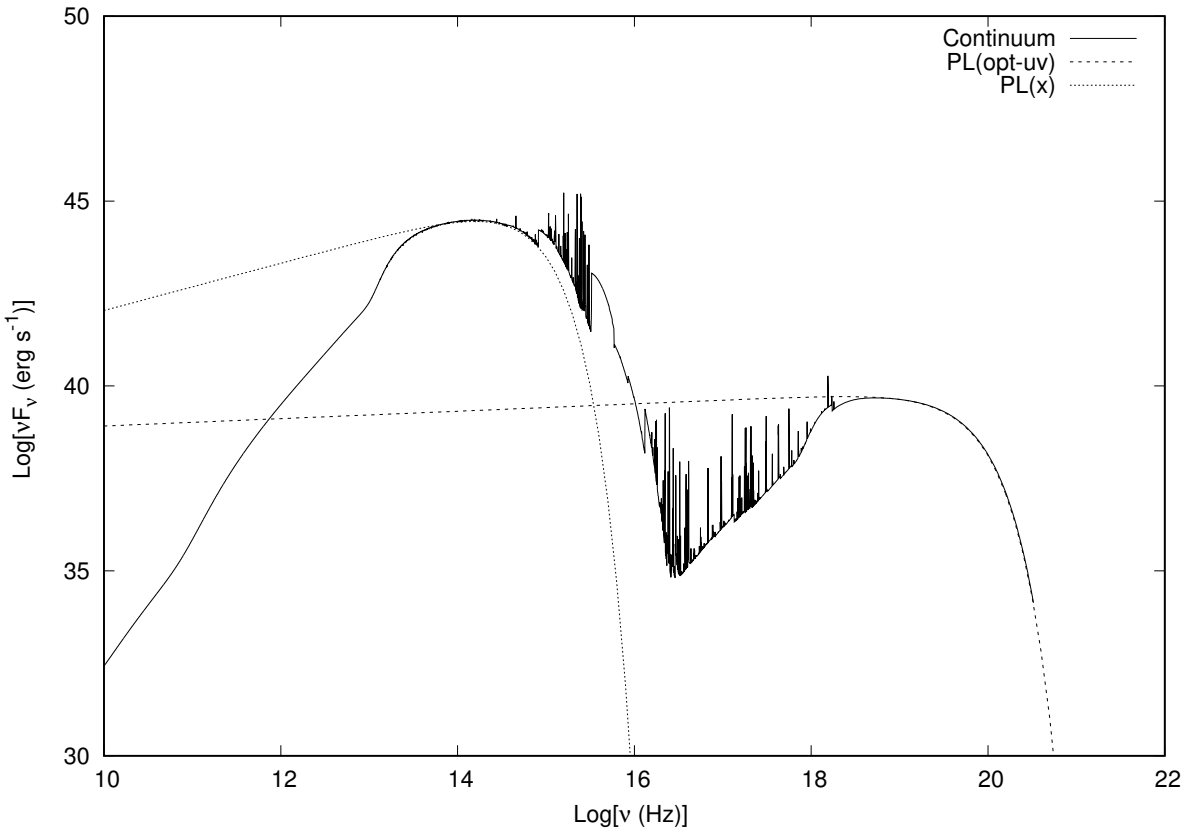

Figure: An example of the spectral energy distribution of the AGN transmitted continuum and line emission produced by CLOUDY: $\mathrm{T_{eff}} = 3.45 \times 10^4\ \mathrm{K}$, $\alpha_{\mathrm{ox}} = -1.6$, $\alpha_{\mathrm{uv}} = -0.36$, $\alpha_{\mathrm{x}} = -0.9$, $\mathrm{n_H} = 10^{11}\ \mathrm{cm^{-3}}$, $\mathrm{N_H} = 10^{24}\ \mathrm{cm^{-2}}$ and $\log(\mathrm{R_{BLR}}) = 17.208$. The two-component power law serves as the incident radiation.

Nicolaus Copernicus Astronomical Center & Center for Theoretical Physics, PAN

SED Modeling

- Starting with values of parameters from Bruhweiler and Verner (2008), we produce the intensities of the broad $\mathrm{Fe_{II}}$ emission lines owing to the corresponding levels of transitions present in CLOUDY 13.04. We calculate the **$\mathrm{Fe_{II}}$ strength**, which is the ratio of $\mathrm{Fe_{II}}$ EW within 4434-4684 Å to broad $\mathrm{H}\beta$ EW

- As a first test we check the dependence of the change in the $\mathrm{T_{eff}}$ to $\mathrm{R_{Fe_{II}}}$ at constant values of $\mathrm{L_{bol}}$, α_{ox}, α_{uv}, $\mathrm{n_H}$ and $\mathrm{N_H}$. We fix the distance to the clouds using the relation by Bentz et. al (2013). The range of Eddington ratio $\left(\frac{\mathrm{L}}{\mathrm{L_{Edd}}}\right)$ for this branch of solutions between 3.45×10^4 K and 5×10^5 K is [0.01244, 2.61247]

$$\left(\frac{\mathrm{R_{BLR}}}{1\ \text{lt-day}}\right) = 10^{\left[1.555+0.542\log\left(\frac{\lambda L_\lambda}{10^{44}\ \mathrm{erg\ s^{-1}}}\right)\right]}$$

Inter-dependence of parameters

Based on the hypothesis, the obtained relation between $\mathrm{R_{Fe_{II}}}$ is heavily affected by the change in the maximum temperature of the BBB-component.

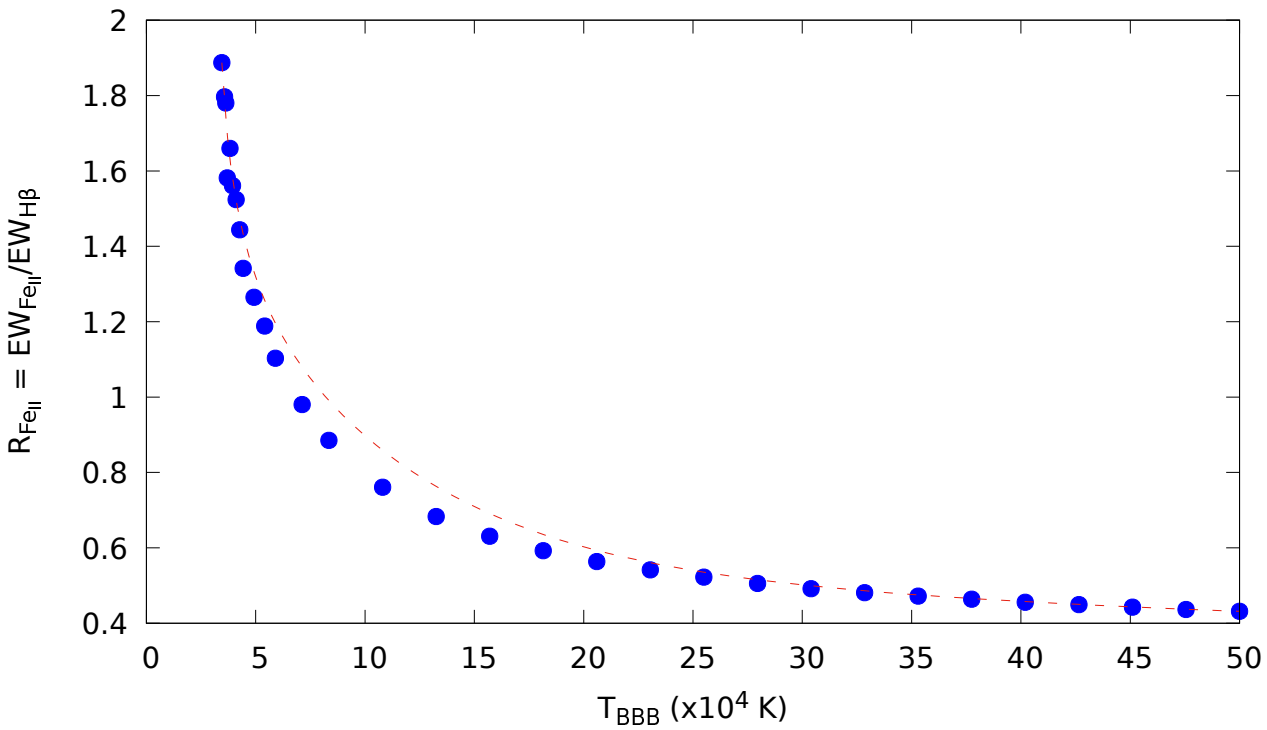

Figure 5: Inter-dependence of the parameters with simple n-degree Bézier curves: $\mathrm{R_{Fe_{II}}}$ - $\mathrm{T_{BBB}}$

Ionized cloud structure

But the plots from the simulations show that - with increase in the maximum disk temperature, there is a fall in the $R_{Fe_{II}}$ (shown by the hyperbolic nature of the plot).

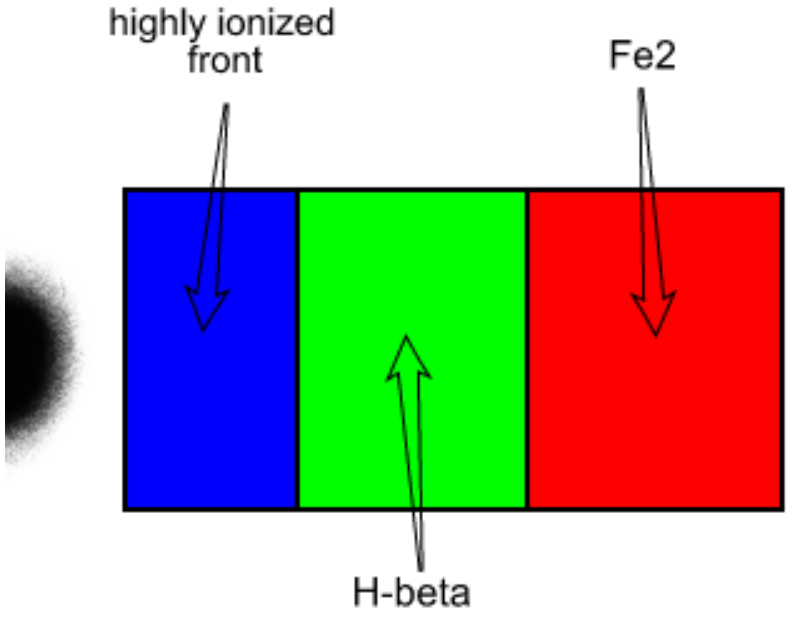

Figure: Different ionizing regions of a cloudlet from the LOC model with plane-parallel geometry

A step further...

- Our initial assumption considered a fixed bolometric luminosity to construct the SED for the opt-UV component. But the trend for $R_{Fe_{II}}$ - T_{BBB} turned out to be exactly opposite!
- We now incorporate a fixed Eddington ratio ($L/L_{Edd} = 1$) and use observationally fitted equations (Czerny & Hryniewicz 2011; Risaliti & Lusso 2017) to compute the luminosity components and their interdependence.

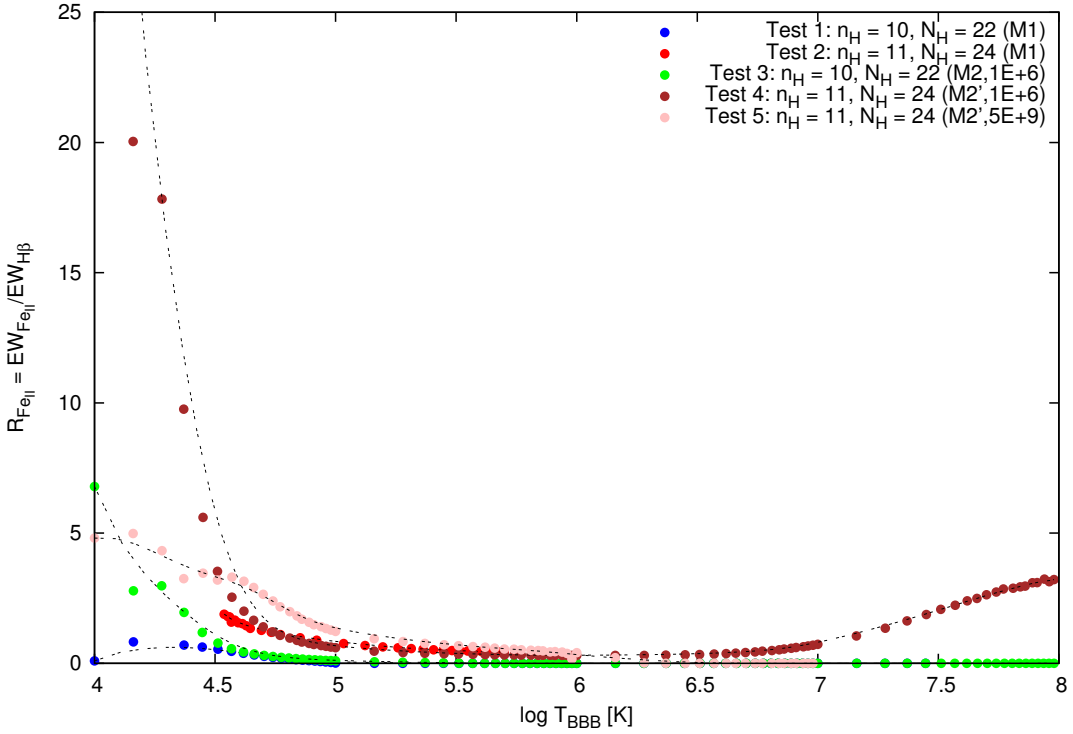

Figure 7: CLOUDY photoionisation trends of $R_{Fe_{II}}$ - T_{BBB}

From Observational Standpoint

- Using the full-GR treatment following the Novikov-Thorne prescription, we simulated an array of SED curves with simultaneous dependence on spin ($0 \leq a \leq 0.998$) and accretion rate ($0.01 \leq \dot{m} \leq 10$). We fitted two observation data (RE J1034+396 (Czerny et al. 2016) and an X-Shooter quasar composite from Selsing et al. 2016) using selected values from these models.

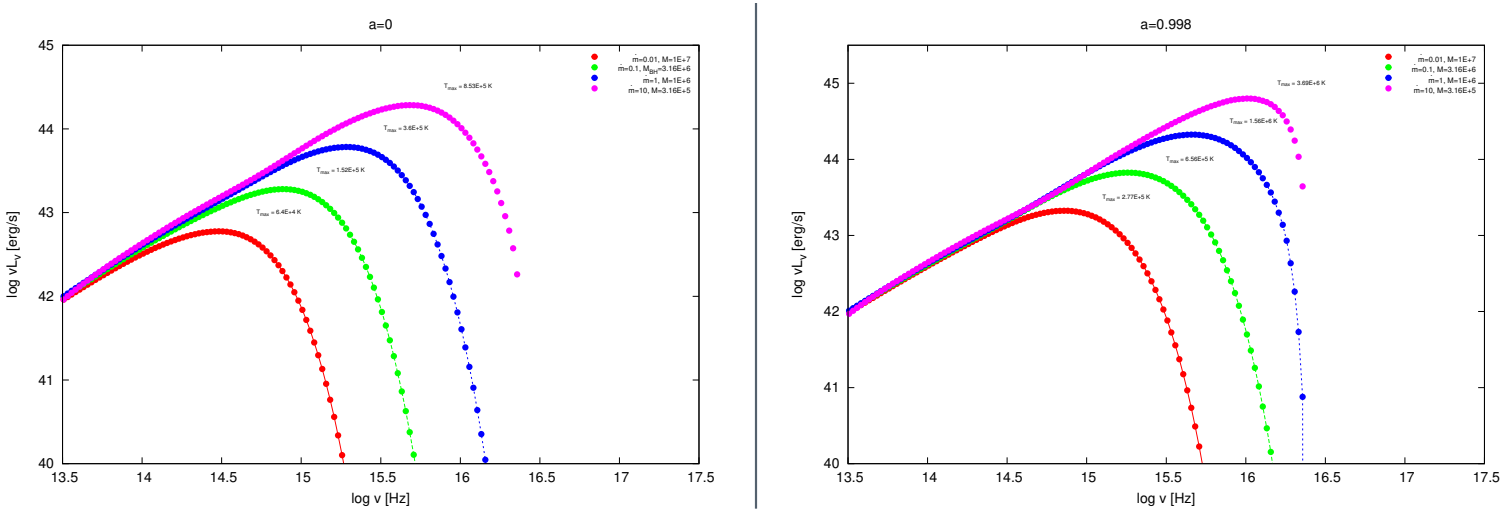

Figure 8: Examples of SEDs with spin-accretion rate modulations under the full-GR modeling (a) a=0, (b) a=0.998

Fitting the Selsing QC

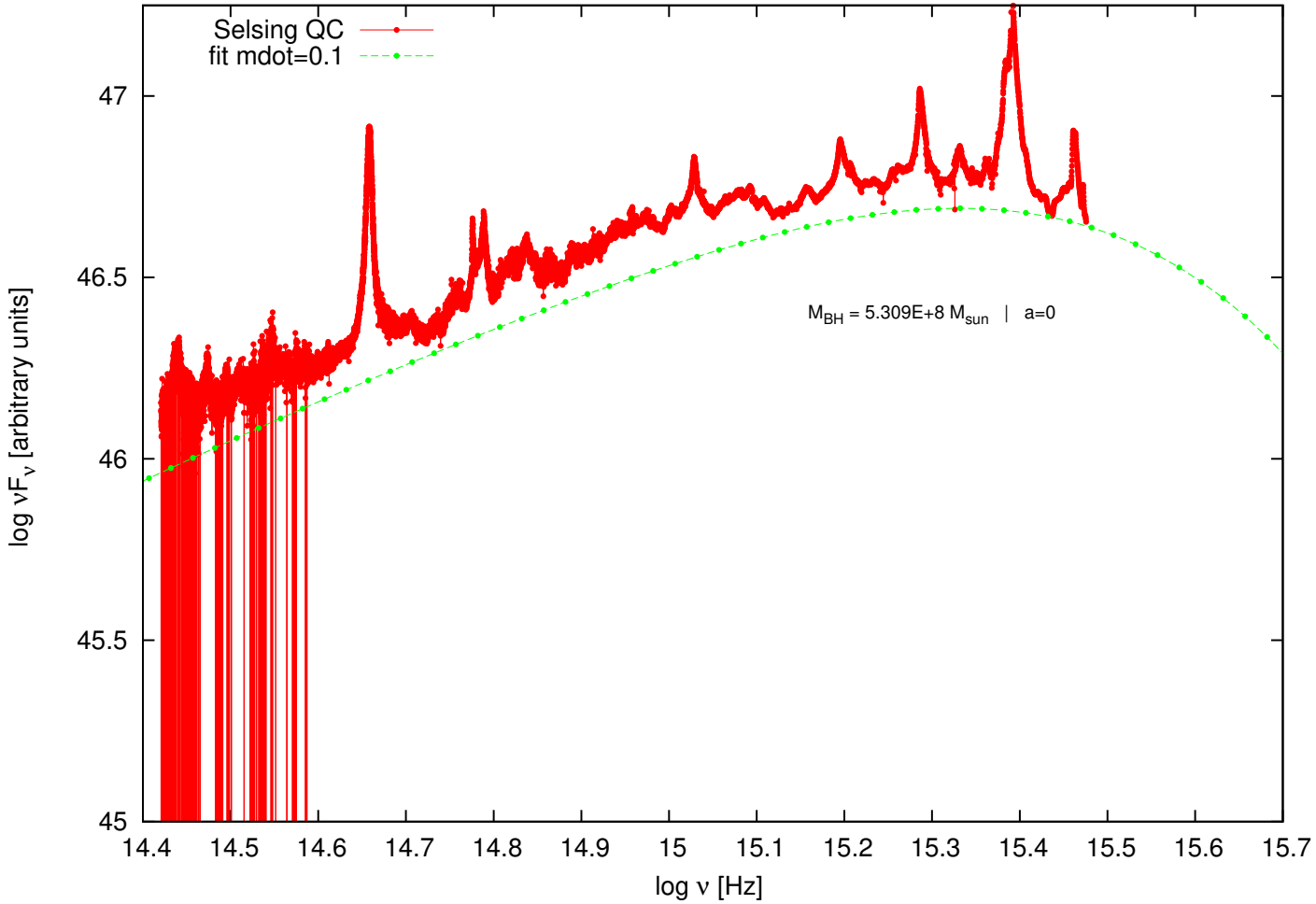

Figure 9: AGN GR-modeling fit over the XShooter quasar composite (a=0, m=0.2, $\mathrm{M_{BH}}$=5.309E+08$\mathrm{M_\odot}$)

Spectra fitting using ray-tracing

- These models are based on $\alpha_{\mathrm{viscosity}}$ and local Keplerian rotation of the disk, as in Shakura & Sunyaev (1973) so they describe a geometrically thin accretion flow with innermost radius located at ISCO (Innermost Stable Circular Orbit) but they include all GR effects, including the spacetime curvature, so the spectra have to be calculated using ray-tracing method.

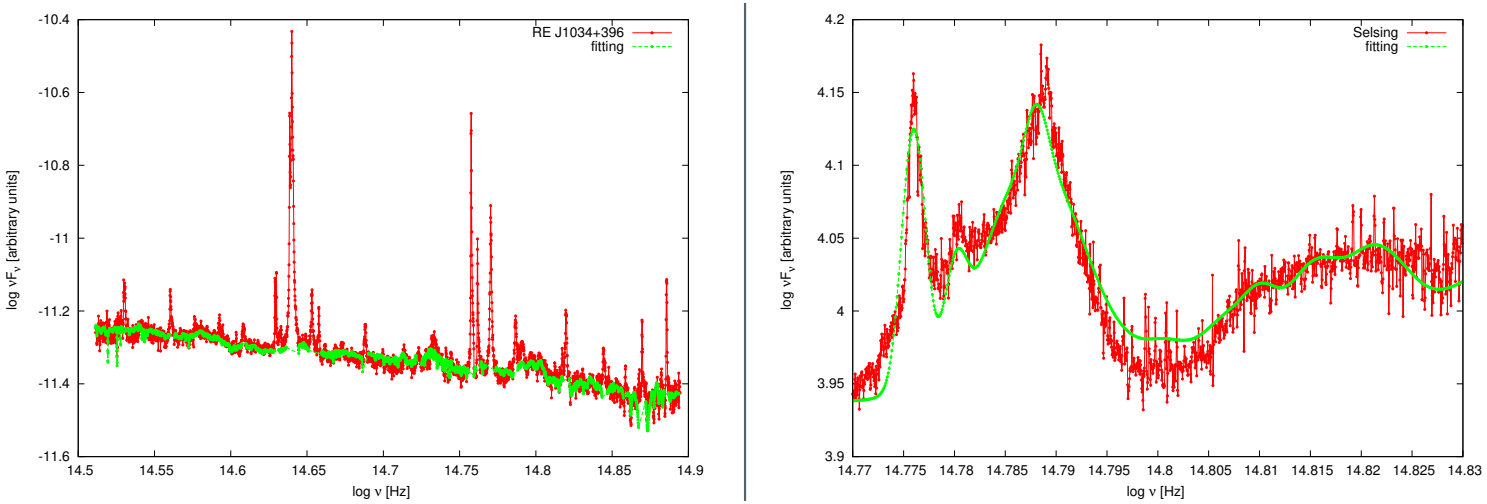

Figure 10: (a) The fit of the a=0 (log M_{BH}=6.55) model to the optical/UV spectrum of RE J1034+396 (Czerny et al. 2016); (b) The least square fit (log M_{BH}=9.65) model to XShooter quasar composite (from Selsing et al. 2016)

A mix of both worlds

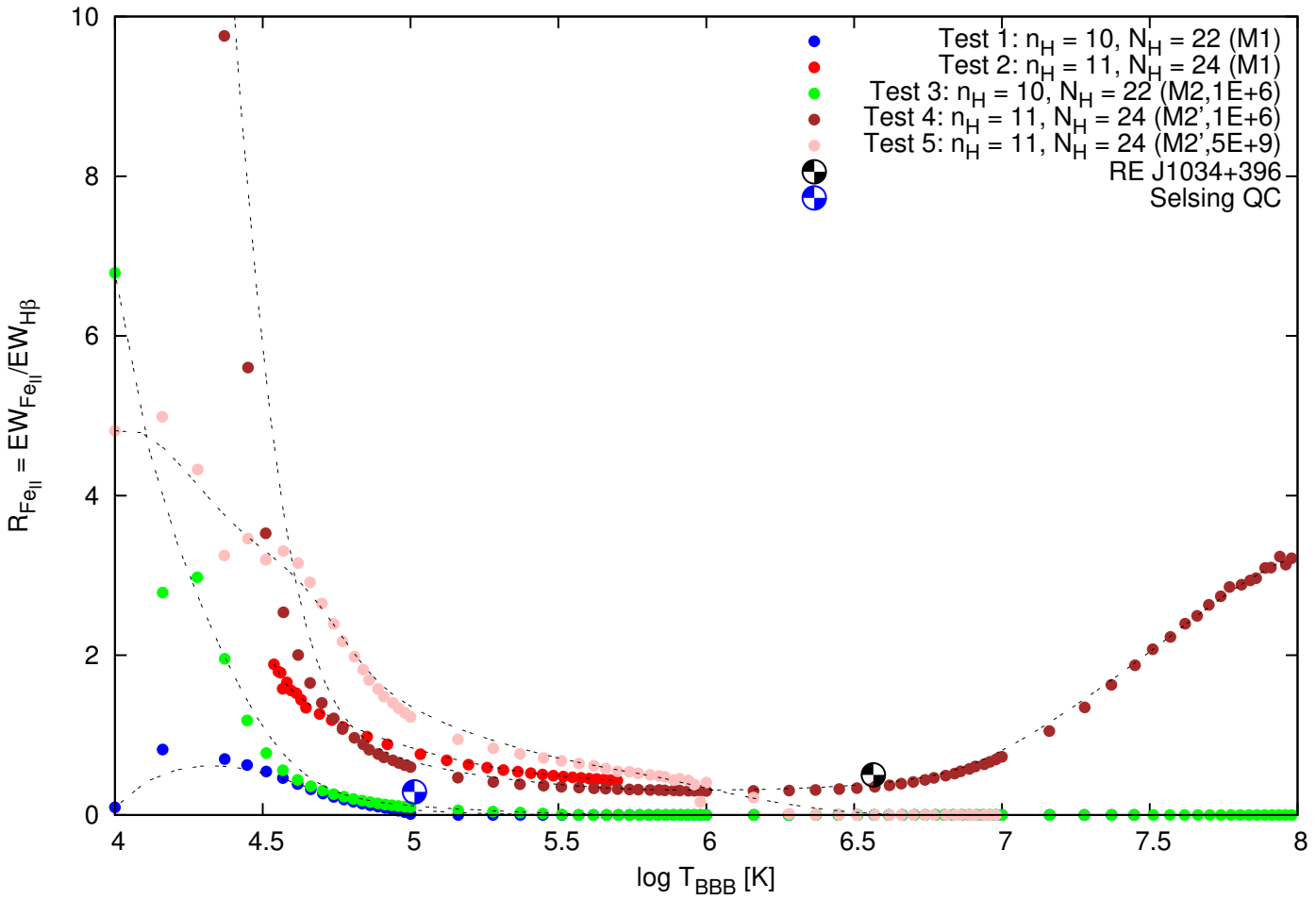

Figure 11: Observational data (RE J1034+396 & Selsing QC) plotted on CLOUDY photoionisation trends of $R_{Fe_{II}}$ - T_{BBB}

Future works (Immediate):

- For the **constant density single cloud**:
  - We need to look more closely the dependence of hydrogen density on the maximum of the disk temperature
  - We intend to incorporate the microturbulence to whose variation the emission flux is sensitive as suggested in Bruhweiler and Verner (2008)
- We will check the $R_{Fe_{II}}$ dependence on other parameters which are used (L_{bol}, α_{ox}, α_{uv}, n_H and N_H)
- We intend to check the mechanism of the formation of Fe_{II} and $H\beta$

Future works (Subsequent):

- For the **constant density LOC model**, we intend to repeat the formalism and check for discrepancies (if any)
- We will reformulate the simulation with the **constant pressure model**
- We need to find a correspondence between disk maximum temperature and the AGN model of a disk + corona with full GR and more complex geometry, and we have to do statistical studies based on samples with known black hole masses
- We will test our theory for the sources with known SED peak position

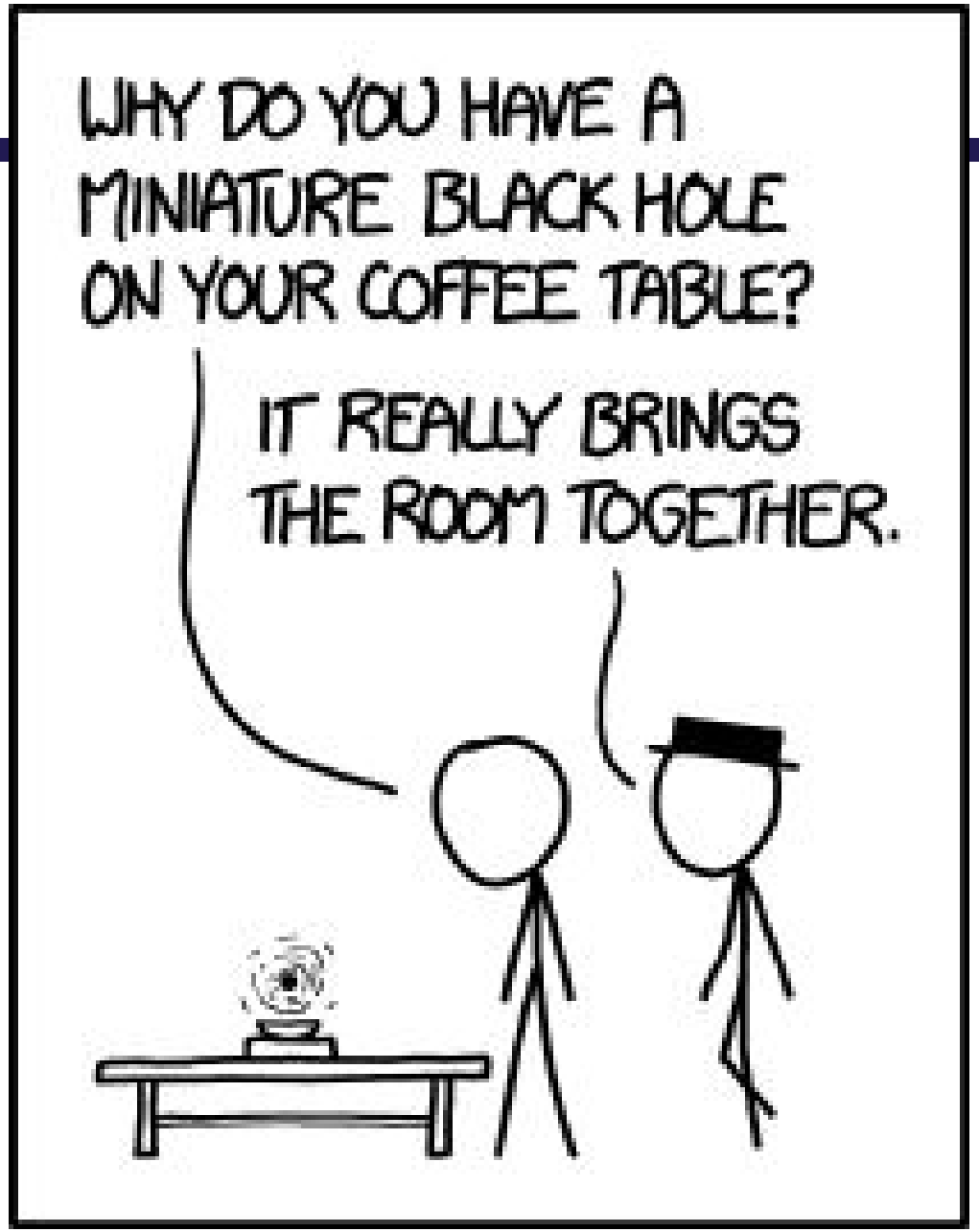

Emissivity plots

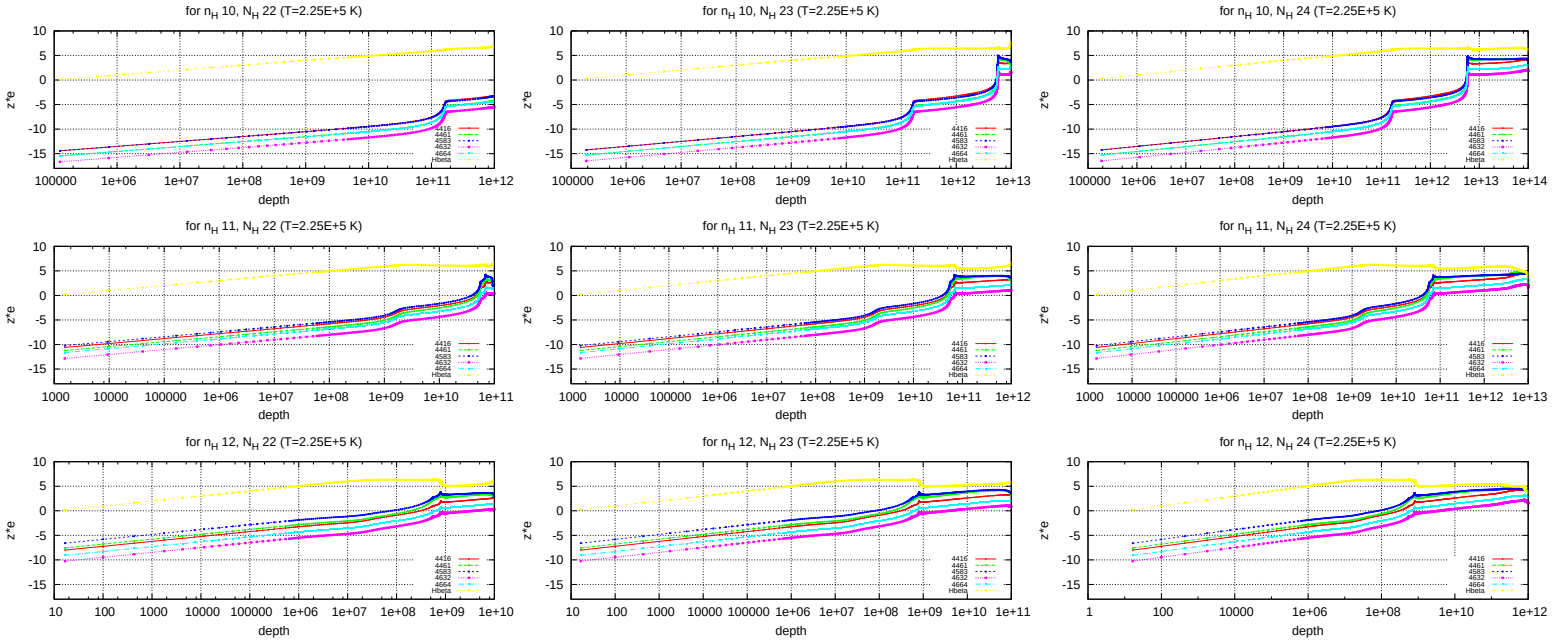

Figure: Regions of Fe_{II} and Hβ based on constant density approximation: T = 2.25 $\times$ 10^5 K

Emissivity plots

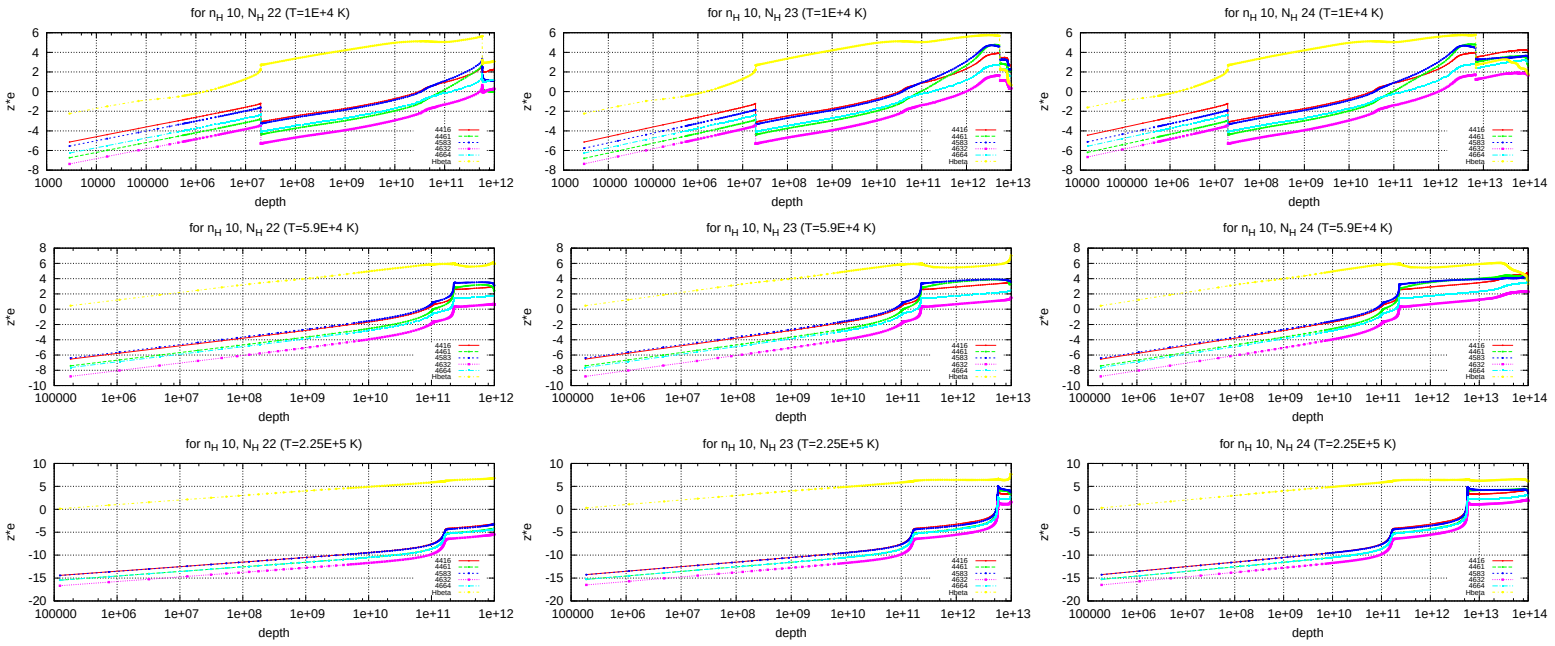

Figure: Regions of Fe_{II} and Hβ based on constant density approximation - comparison at three different T_{BBB} values

Nicolaus Copernicus Astronomical Center
&
Center for Theoretical Physics, PAN

Thermal Instability

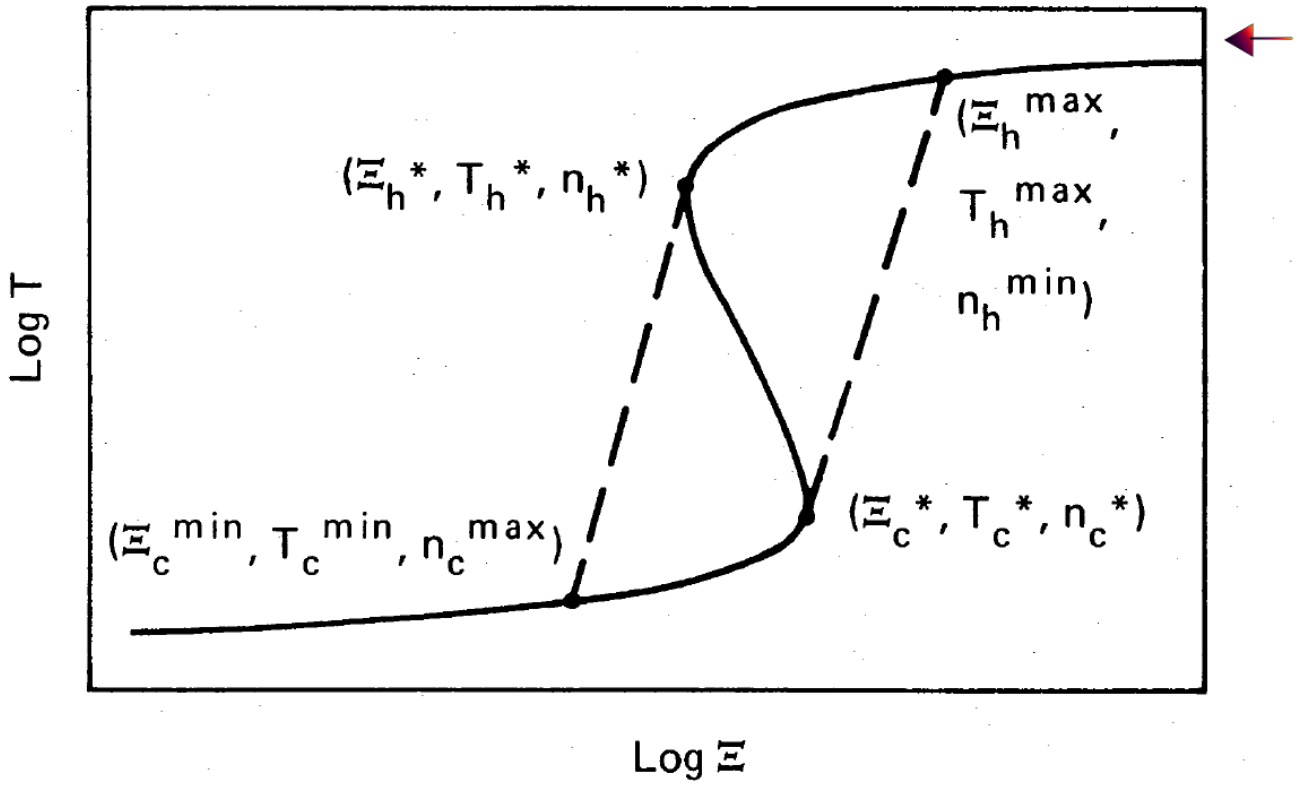

Figure: Schematic drawing of the phase diagram between equilibrium temperature and ionization parameter (Krolik et. al 1981)

$$n_H = \alpha \times T^{\beta}$$

Constant density doesn't work here!

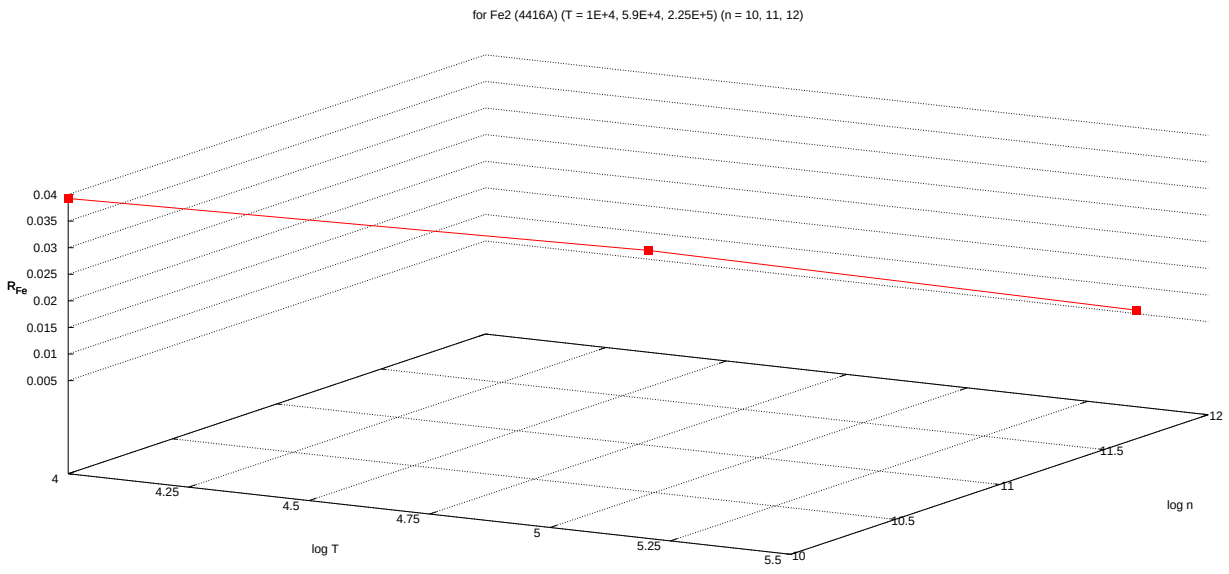

Figure: n_H - maximum disk temperature - $R_{Fe_{II}}$ dependence

$$n_H = 12123.8045 \times T^{1.4791}$$